Analysis of Communication and Control Performance of Multi-Hop IEEE 802.15.4-based WNCSs under Wi-Fi Interference

Muhammad Azeem Khan*†, Yuriy Zacchia Lun*, Piergiuseppe Di Marco*, Aamir Mahmood†, Fortunato Santucci*, and Mikael Gidlund†

*Department of Information Engineering, Computer Science and Mathematics, University of L'Aquila, 67100 L'Aquila, Italy

†Department of Computer and Electrical Engineering, Mid Sweden University, 851 70 Sundsvall, Sweden

*Email: muhammadazeem.khan@graduate.univaq.it, yuriy.zacchialun@univaq.it, piergiuseppe.dimarco@univaq.it, fortunato.santucci@univaq.it, †Email: aamir.mahmood@miun.se, mikael.gidlund@miun.se

***Abstract*—This paper investigates a co-design framework for wireless networked control systems (WNCSs) that integrates multi-hop IEEE 802.15.4-based links under Wi-Fi interference, addressing the challenges of signal-to-interference-plus-noise ratio (SINR) degradation in adverse industrial environments. Multi-hop configurations are essential for extending the operational range and improving SINR in harsh propagation conditions, but they introduce trade-offs in control stability, latency, and computational complexity. We investigate the impact of multi-hop communication on system performance, comparing Bernoulli and Markovian control strategies. Our results demonstrate that multi-hop links effectively extend the operational range and mitigate SINR degradation, but at the cost of increased latency and computational cost. We analyze the spectral radius of the system stability verification matrix and control costs for Bernoulli and Markovian control strategies, illustrating that network latency and hop counts can be balanced while maintaining the stability of the multi-hop WNCS. Markovian strategy, although more computationally intensive, outperforms Bernoulli strategy under high interference, offering a robust solution for industrial WNCSs. The proposed framework provides a practical approach for deploying reliable WNCSs in interference-prone environments.**

***Index Terms*—Multi-hop wireless communication, Wireless Network Control Systems, Industrial Internet of Things (IIoT).**

I. Introduction

In recent years, the industrial Internet of things (IIoT) has emerged as a transformative force across various sectors, including manufacturing, energy, transportation, and healthcare. At the heart of IIoT lies wireless networked control systems (WNCSs), which provide flexible, scalable, and cost-effective solutions for real-time monitoring and control of industrial assets. These systems rely on wireless communication to connect distributed sensors, actuators, and controllers, enabling seamless data exchange and remote operation. However, deploying WNCSs in industrial environments often involves overcoming significant challenges, such as signal degradation, increased latency, and interference—particularly in unlicensed frequency bands like the 2.4 GHz industrial, scientific, and medical (ISM) band. These challenges are further exacerbated when multiple wireless standards, such as IEEE 802.11 (Wi-Fi) and IEEE 802.15.4 (used in WirelessHART and ISA 100.11a), operate in close proximity, leading to interference, degradation of the signal-to-interference-plus-noise ratio (SINR), and ultimately, packet losses.

A critical challenge in WNCS design is the interplay between the communication and control subsystems. As highlighted in [1], the mutual impact of these subsystems on system performance necessitates co-design approaches to ensure stability and efficiency. For example, [2] proposes a WNCS architecture for distributed control under Bernoulli packet loss, while recent studies [3], [4] have explored finite-state Markov channel (FSMC) models for control and estimation. Modern research has also focused on transmission scheduling for state estimation under various packet loss models [5] and on trade-offs between latency and reliability [6]. Similarly [7] investigated the balance between communication delay and packet reliability for state estimation, proposing optimized coding strategies that incorporate finite blocklength coding to mitigate performance degradation caused by unreliable channels. [8] introduced a communication-control co-design framework for wireless edge industrial systems, where computationally intensive tasks like robotic perception are offloaded to an edge server. Their modular deep reinforcement learning (DRL) framework optimizes network quality of service (QoS) while maintaining control stability, demonstrating that adaptive scheduling and QoS-aware policies can significantly reduce communication overhead.

Interference from coexisting wireless technologies presents another major challenge. Analytical models have been developed to characterize interference and support coexistence analysis [9]–[11]. However, many of these models assume saturated conditions with equidistant interfering devices, which may not accurately reflect real-world industrial environments. For instance, studies such as [12] have examined the impact of Wi-Fi on IEEE 802.15.4 networks, identifying packet collisions and losses as primary issues. Techniques like adaptive frequency hopping and dynamic spectrum access have been proposed to mitigate interference [13], but designing WNCSs that maintain stability under dynamic interference remains a complex task, underscoring the need for precise interference modeling tailored to industrial settings.

Multi-hop communication is essential for extending the coverage of IIoT deployments, particularly in large-scale industrial environments. However, extending single-hop packet loss models to multi-hop networks requires accounting for factors such as network topology, routing protocols, and varying traffic loads [1]. The impact of multi-hop latency on control system stability has been analyzed in [14], [15], revealing how delays can degrade performance. To address latency sensitivity in industrial applications, strategies like predictive control and delay compensation have been proposed, although these approaches often assume static network conditions, which may not hold in dynamic IIoT environments [16]. Balancing control stability and communication delay in multi-hop WNCSs typically relies on Bernoulli and Markovian models for handling packet losses. While the Bernoulli model assumes independent and identically distributed (i.i.d.) losses, it fails to capture bursty loss patterns [17]. In contrast, Markovian models account for temporal correlations, offering a more accurate representation of wireless channels and better prediction of control performance, especially in interference-prone settings [18]. Recent work [19] has introduced an analytical framework that co-designs WNCSs using IEEE 802.15.4-based links under Wi-Fi interference, incorporating FSMC models to capture bursty packet losses more effectively than traditional Bernoulli models, thus enhancing stability and control performance in single-hop setups.

The design of WNCSs has been further transformed by advancements in the IIoT domain. A comprehensive overview of IIoT challenges and opportunities is provided in [20], which emphasizes the importance of real-time performance, energy efficiency, and interoperability in industrial wireless networks. This work also highlights the role of multi-hop wireless sensor networks in extending communication range without sacrificing reliability. Alongside this, [21] examines the future of industrial communication networks in the IoT era, focusing on the integration of time-sensitive networking (TSN) and 5G technologies to achieve deterministic communication in industrial automation. This integration enables seamless connectivity across heterogeneous industrial networks.

Significant attention has also been directed toward integrated approaches for scheduling and routing in multi-hop control networks. One notable contribution is [22], which proposes a satisfiability modulo theory (SMT)-based framework for optimizing control scheduling and ensuring timely message delivery in resource-constrained wireless environments. Complementing this, [23] introduces a high-performance wireless connectivity solution for closed-loop control over multi-hop networks. This solution employs control-aware bidirectional scheduling, cooperative retransmission, and low-overhead signaling to achieve low-latency and high-reliability communication in Industrial IoT applications.

Stochastic predictive control under unreliable sensor and control channels has also been a focus of extensive research. In [24], a Kalman-filter-based estimation approach is proposed to compensate for packet dropouts, ensuring Lyapunov stability even when control transmissions experience Bernoulli erasures. This approach is particularly relevant for real-time industrial applications. Additionally, [25] explores a machine learning-based predictive control approach that utilizes gaussian process regression (GPR) to predict missing control states and actions. Their age-of-information (AoI)-aware scheduling algorithm dynamically prioritizes transmissions, optimizing network-wide control stability while minimizing wireless resource consumption.

Despite these advancements, a comprehensive framework that integrates multi-hop communication and precise interference modeling in WNCSs remains an open challenge. Many studies default to Bernoulli packet loss models, thereby overlooking the need for more suitable wireless link abstractions. Large-scale IIoT deployments, which often require multi-hop communication, face the dual challenge of cascaded packet losses and increased latency, both critical factors in maintaining control stability and performance in time-sensitive applications. To address these issues, our work proposes a co-design framework that adapts single-link modeling approaches [19] to a multi-hop setting. By leveraging multi-hop communication, our framework achieves greater operational range and improved SINR compared to direct links over the same distance, thus supporting system stability.

Our study focuses on delay-sensitive applications that utilize a static scheduler with pre-computed transmission times, eliminating variability due to dynamic scheduling. In our analysis, we do not consider retransmissions because their inherent latency is unaffordable in time-constrained scenarios. Future work may explore the impact of limited retransmissions based on the number of hops and the system's sampling rate.

The key contributions of this paper are as follows:

1) **SINR Degradation Analysis:** We analyze the effects of SINR degradation on stabilization over direct links for both control strategies, revealing that beyond certain distances, SINR loss hinders stabilization and increases control costs.
2) **Stabilization Conditions:** We identify conditions under which multi-hop configurations enable stabilization while considering computational load and network latency constraints.
3) **Validation:** We validate our approach through simulations on an inverted rotary pendulum system, demonstrating its effectiveness for industrial applications under challenging interference conditions.

The remainder of this paper is organized as follows. Section II describes our proposed system model. Section III outlines the impact of the multi-hop framework, and Section IV presents the simulation setup and results. Finally, Section V concludes with key findings and future research directions.

II. System Model

In this section, we describe the system model used to analyze the performance of WNCSs in industrial environments, particularly focusing on multi-hop communication.

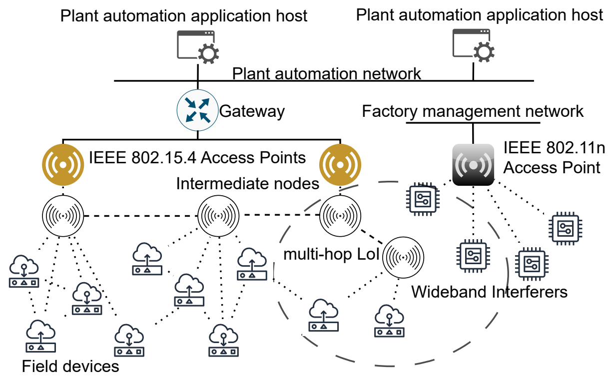

Fig. 1. Illustration of a multi-hop IEEE 802.15.4 plant automation network coexisting with an IEEE 802.11n network, with the link of interest (LoI) subject to Wi-Fi interference in the shared 2.4 GHz ISM band.

A. Network Architecture

Our WNCS employs IEEE 802.15.4-based communication standards (such as WirelessHART and ISA 100.11a) operating in the 2.4 GHz ISM band. The field devices, which include sensors and actuators, are deployed in an incomplete mesh topology, communicating with the controller via multiple relay nodes as shown in Fig.1. The controller processes sensor measurements and sends control commands back to the actuators via the same multi-hop path. This close loop system operates with a fixed sampling period T_s, representing the maximum allowable end-to-end (E2E) delay to maintain the stability of the control system.

Each wireless link in the control network is modeled as a time-varying fading channel, where packet loss is influenced by both network congestion and external interference. The network follows a time-division multiple access (TDMA) scheme to minimize collisions and ensure deterministic communication. This setup reduces SINR degradation from long single-hop transmissions by introducing shorter intermediate hops. However, due to the presence of multiple hops, E2E latency and packet loss pose significant challenges to control stability.

B. Signal-to-Interference-plus-Noise Ratio (SINR)

SINR is a key metric that defines the quality of a wireless communication link by comparing the desired signal's power to the combined power of interference and noise. In industrial WNCSs, SINR directly impacts the reliability and stability of control signals, particularly in environments where interference from IEEE 802.11 (Wi-Fi) networks is dominant. The SINR can be expressed as

$$\gamma_t = \frac{S_c}{N_0 + I_s}, \tag{1}$$

where S_c represents the signal power spectral density (PSD), N_0 is the noise PSD, and I_s is the interference PSD.

1) Signal Power: The signal PSD S_c is determined from c_t in (2), which accounts for the desired signal strength, including path loss and shadow fading. The term c_t is defined as:

$$c_t = \sqrt{E_c}\alpha_s e^{\frac{\chi_s(t)}{2}}, \tag{2}$$

where E_c is the chip energy, α_s represents the path loss coefficient, and $\chi_s(t)$ accounts for shadow fading and residual power control error. The S_c is given by $S_c = c_t^2$.

2) Noise Power: The noise power P_{noise} is primarily thermal noise, modeled as additive white Gaussian noise (AWGN), with a PSD of $N_0 = -174\,\text{dBm/Hz}$. For the IEEE 802.15.4 system, which operates with a bandwidth $B = 2\,\text{MHz}$, the total noise power is given by $P_{\text{noise}} = N_0 B$.

3) Interference Power: The interference PSD I_s accounts for the cumulative interference from multiple coexisting Wi-Fi devices. The interference experienced by the WNCS is influenced by factors such as the density of Wi-Fi devices, the medium access mechanism (basic access or RTS/CTS), and the number of active devices near the receiver. As the number of interfering devices increases, the interference power spectral density I_s increases, leading to a lower SINR. For a detailed analysis of SINR under Wi-Fi interference, refer to [19].

C. Multi-Hop Communication and Latency Analysis

In a multi-hop network, data from field devices is relayed to the controller through multiple intermediate nodes. Let $N = \{n_1, n_2, \ldots, n_M\}$ representing the set of relay nodes, with M denoting the total number of hops. The total latency experienced by a packet is the aggregate of propagation, transmission, and processing delays across all hops. Thus, the E2E delay T_{E2E} over L hops can be expressed as

$$T_{E2E} = \sum_{\ell=1}^{L} \left(T_{prop}(\ell) + T_{tx}(\ell) + T_{proc}(\ell) \right), \tag{3}$$

where $T_{prop}(\ell)$, $T_{tx}(\ell)$, and $T_{proc}(\ell)$ are the propagation, transmission, and processing delays at the ℓ-th hop.

1) Propagation Delay: $T_{prop}(\ell)$ is calculated based on the distance d_ℓ between adjacent nodes and the speed of light c

$$T_{prop}(\ell) = \frac{d_\ell}{c}. \tag{4}$$

2) Transmission Delay: $T_{tx}(\ell)$ is determined by the frame length f_ℓ and the data rate R of the link

$$T_{tx}(\ell) = \frac{f_\ell}{R}. \tag{5}$$

For IEEE 802.15.4 link operating at 250 kbps, the frame length is computed based on the protocol and the number of control variables, defined in the model.

3) Processing Delay: $T_{proc}(\ell)$ accounts for the time each relay node requires to process and forward the packet as illustrated in Fig.2. The typical values for IEEE 802.15.4 networks range around 3.2 ms for beacon-enabled networks and 2.9 ms for non-beacon networks [26].

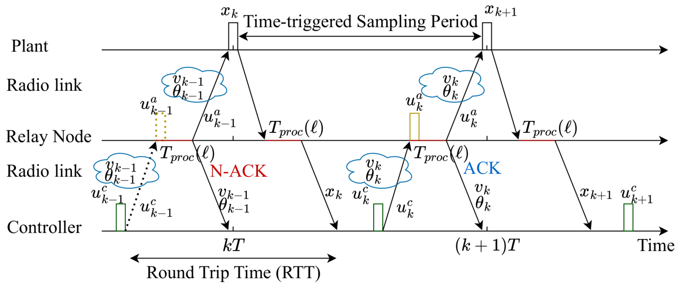

Fig. 2. The timing diagram for a closed-loop system with time-triggered sampling and potential packet losses on multi-hop radio link between the controller and plant. At time step $k-1$, the control packet containing u^c_{k-1} is corrupted during transmission. The receiver detects this error, discards the message, and sends a N-ACK signal indicating that $\nu_{k-1} = 0$. This packet also contains the estimated state of the link, θ_{k-1}. At time step k, the control signal u^c_k is received correctly, and an ACK signal $\nu_k = 1$ is sent to the controller, together with the new estimation θ_k of the link's state. RTT represents the round-trip time for a command from the controller to the plant and back, with $T_{RTT} \approx 2 \times T_{E2E}$.

4) Impact on Control Systems: In industrial WNCSs, ensuring that latency remains within a critical threshold is crucial for maintaining stability. In this study, the maximal allowable delay is set within the sampling period T_s; therefore, the total E2E delay T_{E2E} must satisfy $T_{E2E} \leq T_s$. Exceeding this limit, where $T_{E2E} > T_s$, results in system instability and degraded control performance.

D. Retransmissions and Scheduling Considerations

This study focuses on delay-sensitive applications that utilize a static scheduler, where transmission times are predetermined, eliminating scheduling variability. This approach is a well-established and classical method in many industrial applications, particularly those that prioritize time-sensitive operations.

When it comes to retransmissions, their role depends on the layer of the protocol stack being considered. At the transport layer, UDP is preferred over TCP in time-critical applications as it does not retransmit lost packets, avoiding delays that could disrupt real-time operations. However, at the link layer, retransmissions may still occur, but they are usually configurable. For example, we can choose to disable retransmissions entirely, allow a single retransmission, or permit multiple retransmissions up to a certain limit.

Given these constraints, retransmissions are not considered in our current analysis. End-to-end retransmissions are excluded as they significantly increase latency, making them unsuitable for time-sensitive applications. On the other hand, link-layer retransmissions can be incorporated into the model, provided they occur within the allocated time slot and do not exceed the deadline for frame recognition. For now, we prioritize timely data delivery over packet recovery to maintain system responsiveness and information freshness. Future work may explore the feasibility of limited retransmissions, determining the maximum allowable retransmissions based on network hop count while ensuring they occur within a single sampling period to prevent timing disruptions.

E. Control System Model

In WNCSs with acknowledgment of transmission outcomes, the separation principle enables the independent design of the remote system state estimator and the controller [4]. This is particularly important because the remote controller observes the channel state with a one-time-step delay, creating challenges in optimal control over fading channels. As a result, even if the system remains detectable under the same channel conditions, it may not always be controllable, making the controller design the main challenge in wireless output-feedback control. Hence, this section focuses on the optimal state-feedback problem, considering that it is also a vital challenge in output-feedback control over fading channels.

The control system is a linear discrete-time system with packet losses between the controller and the actuator, modeled as either a Bernoulli or FSMC process. The objective is to minimize the infinite-horizon quadratic cost function (6), as formulated in [19], maintaining system stability despite stochastic packet drops and constant actuation delays of less than one sampling period.

$$J = \lim_{N\to\infty} \frac{1}{N} \mathbb{E}\left[\sum_{k=0}^{N} \left(\xi_k^T Q_1 \xi_k + u_k^T R u_k\right)\right], \tag{6}$$

where Q_1 and R are positive-semidefinite and positive-definite state and input weighting matrices respectively, that balance state regulation against control effort.

From [27, Sec. 4.3.4], the discrete-time system dynamics are given by

$$\xi_{k+1} = A_1 \xi_k + B_1 u_{k-1} + B_2 u_k + w_k, \tag{7}$$

where ξ_k is the system state vector, u_k is the control input at the actuator, A_1, B_1, and B_2 are constant matrices, and w_k is Gaussian white noise with zero mean and covariance Σ_w.

Under the zero-order hold, the constant continuous-time system state and input matrices F and G define the discrete-time matrices A_1, B_1, and B_2. For any time interval λ, let

$$\mathcal{A}(\lambda) = e^{F\lambda}, \quad \mathcal{B}(\lambda) = \int_0^{\lambda} e^{F\varsigma} d\varsigma G, \tag{8}$$

so that

$$A_1 = \mathcal{A}(T_s), \quad B_1 = \mathcal{A}(T_s - T_{E2E})\mathcal{B}(T_{E2E}), \tag{9}$$

and

$$B_2 = \mathcal{B}(T_s - T_{E2E}). \tag{10}$$

The input u_k is subject to packet losses, modeled as

$$u_k = \nu_k \hat{u}_k, \tag{11}$$

where $\hat{u}_k$ is the command from the controller, and ν_k is a random variable indicating packet reception (1 if successful, 0 otherwise) [19]. We investigate two cases of packet loss:

1) Control under Bernoulli Packet Loss: When packet losses are Bernoulli distributed, they occur independently at each time step. The controller's information set is

$$\mathcal{F}_k = \{\xi_k, \nu_{k-1}\}, \tag{12}$$

where ξ_k is the current system state and ν_{k-1} indicates the success of the previous transmission.

2) Control under FSMC Packet Loss: With Markov packet losses, the loss probability depends on the channel state. The controller's information set expands to

$$\mathcal{G}_k = \{\xi_k, \nu_{k-1}, \theta_{k-1}\}, \tag{13}$$

where θ_{k-1} reflects the channel state at the last time step, capturing temporal correlations [19].

Both control strategies aim to minimize (6) while maintaining system stability. Mean-square stability is achieved if the second moment of the system state converges to zero as $k \to \infty$.

To represent the system dynamics in the standard state-space form without the previous input term $B_1 u_{k-1}$, we follow [27, Sec. 4.3.4] to define the augmented system as

$$x_{k+1} = Ax_k + Bu_k + Hw_k, \tag{14}$$

$$x_k = \begin{bmatrix} \xi_k \\ u_{k-1} \end{bmatrix},\ A = \begin{bmatrix} A_1 & B_1 \\ 0 & 0 \end{bmatrix},\ B = \begin{bmatrix} B_2 \\ I \end{bmatrix},\ H = \begin{bmatrix} I \\ 0 \end{bmatrix}, \tag{15}$$

where I indicates the identity matrix of appropriate size. Notice from (11)–(13) that ν_{k-1} and thus u_{k-1} are known to the controller at time step k. Consequently, we can perform the system analysis on the augmented system, substituting ξ_k with x_k in (12)–(6) and Q_1 with Q in (6).

$$Q = \begin{bmatrix} Q_1 & 0 \\ 0 & 0 \end{bmatrix}. \tag{16}$$

III. Impact of Multi-Hop Framework

This section examines how adding relay nodes to extend communication range impacts critical control metrics. We analyze the relationships among SINR, spectral radius, control costs, and E2E latency across varying hop counts to assess the scalability and constraints of multi-hop WNCSs.

A. Control Strategies and Stability Metrics

The spectral radius (ρ) of the system stability verification matrix, defined as the largest absolute value among its eigenvalues [28], serves as a key stability indicator in control systems. When $\rho < 1$, the system is stable, however, as ρ approaches or exceeds 1, instability and increased control costs are expected. Under Bernoulli control, packet losses are assumed to be independent. Still, as the number of hops grows, the ρ under Bernoulli can exceed 1, limiting the strategy's ability to stabilize the plant. The Markovian control strategy, however, incorporates temporal correlations in packet losses and partitions the channel into finite states based on SINR and packet error rate (PER). This strategy enables better performance under bursty packet losses by adapting to channel conditions across multiple hops. The Markovian strategy can maintain stability over more hops by leveraging these state-dependent packet loss probabilities. Nonetheless, this requires detailed knowledge of the channel states at each hop, introducing computational complexity as the state space expands exponentially with additional hops.

B. Impact of Extended Range by Relay Nodes

As the distance between the source and destination grows, SINR reduces due to increased path loss and interference, increasing the packet loss probability. When the probability of receiving a packet falls below the critical control packet arrival probability ν_c, the ρ of the system stability verification matrix surpasses 1, resulting in higher control costs and instability. To compute ν_c, we examine the unstable eigenvalues of the state matrix A, which reflect the system's behavior without control intervention. Stability requires ν_c to be above a threshold based on these eigenvalues, ensuring control input counteracts system instability. The exact value of ν_c is typically determined through numerical methods, like solving a linear matrix inequality (LMI) optimization problem [19].

Relay nodes are introduced to extend the communication range and mitigate SINR degradation, effectively transforming the direct link into a multi-hop one. While this approach introduces additional challenges as:

- *Increased Latency:* Each additional hop adds propagation, transmission, and processing delays, increasing E2E latency.
- *Centralized Scheduling:* Under the centralized TDMA, multi-hop links require precise scheduling of transmission time slots to limit the E2E latency.
- *Rising Control Costs:* With more hops, the average control costs for both Bernoulli and Markovian strategies increase, leading to higher PER and system complexity.
- *Stability Constraints:* As hop count increases, the ρ of the Bernoulli strategy exceeds 1, limiting its ability to stabilize the system. However, the Markovian strategy can maintain stability over a greater number of hops by adapting to state-dependent loss probabilities [19].

C. Computational Complexity and Delay Constraints

The Markovian strategy faces exponential growth in the number of E2E channel states as each hop introduces a unique SINR and PER-based states. Consequently, the controller must process the expanded state space, increasing computational demands. This complexity, coupled with cumulative delays from all hops, can challenge the system's ability to respond within the control sampling period T_s.

The E2E latency, must not exceed the maximum allowable delay. Delay constraints limit the feasible number of hops, creating a trade-off between extending range and maintaining control performance. In practice, this trade-off defines the operational bounds for the multi-hop WNCS, where stability, computation demands, and latency requirements converge.

By examining ρ, communication range, SINR, control costs, and delay across various hop counts, this study provides insights into balancing stability, computational demands, and

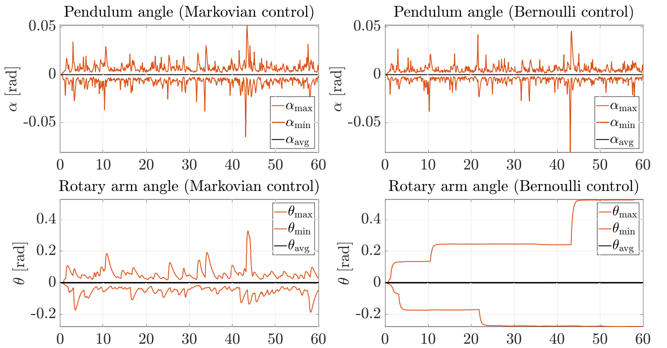

Fig. 3. State evolution of the inverted rotary pendulum under interference from 15 active Wi-Fi devices on the link of interest. Solid lines show the extreme observed behavior, with all traces contained within the area bounded by these lines.

latency in multi-hop WNCSs. The resulting framework highlights critical considerations for maintaining robust control performance across scalable multi-hop networks.

IV. Results and Discussion

This section presents simulation results, focusing on average SINR, E2E delay, and the spectral radius (ρ) of the stability matrix for Bernoulli and Markovian control strategies. To evaluate the impact of interference on multi-hop WNCS performance, we model a challenging control scenario involving an inverted rotary pendulum, where the controller aims to maintain an upright position. The system state includes the rotary arm and pendulum angles with their angular velocities, applicable for small deviations up to 10° (0.175 radians). The critical packet arrival probability under Bernoulli loss is $\nu_c = 0.811$ with zero-order hold sampling at $R = 10\,\text{Hz}$ (WirelessHART, operates at the same frequency). We conducted 250,000 Monte Carlo simulations of closed-loop balancing control for the inverted rotary pendulum using both Markovian and Bernoulli control strategies. Each trace lasted 60 s, recording channel-state evolution and successful control packet arrivals, achieving 60 s of balancing control as shown in Fig. 3.

The number of hops in the IEEE 802.15.4-based network between the controller and the plant defines the distance, with the communication operating on channel 11 at 10 dBm transmission power. The propagation environment is line-of-sight without obstacles. The interfering network uses the RTS/CTS (request to send/clear to send) medium access mechanism. In total, 15 Wi-Fi devices generate interference at 10 m from the IEEE 802.15.4-compliant receiver. Each Wi-Fi device transmits on channel 1 at 10 dBm, with a slot time $T_E = 20\,\mu\text{s}$ and Wi-Fi payload transmission time $T_P = 10\,\text{ms}$.

The system is subject to Gaussian white noise with covariance matrix $\Sigma_w = 2.5$. We analyze the performance of both mode-independent and mode-dependent state-feedback control laws in the presence of Wi-Fi interference. The results show varying levels of control performance, with Bernoulli control capable of stabilizing the system in some cases, while the Markovian control strategy proves more effective in multi-hop

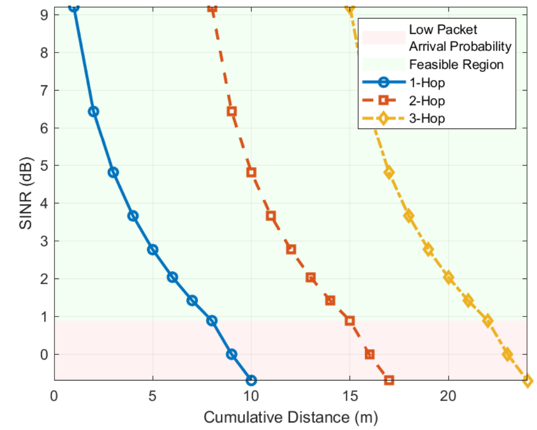

Fig. 4. SINR vs cumulative distance in multi-hop settings.

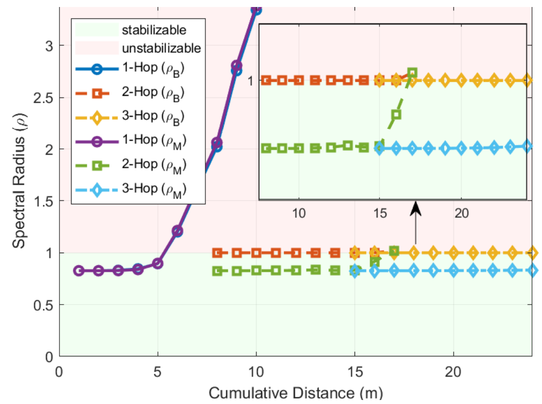

Fig. 5. Spectral radius (ρ) vs cumulative distance in multi-hop settings.

scenarios due to its ability to partition the channel states and better estimate packet loss.

In the one-hop configuration shown in Fig. 4, the SINR decreases substantially as the distance between the source and destination increases. Starting at a distance of 1 m, the SINR is about 9 dB, but it drops to -0.3 dB at 10 m. This highlights the difficulty in maintaining stability at longer distances due to signal degradation. The spectral radius ρ of the system stability verification matrix, as shown in Fig. 5, increases with decreasing SINR, indicating higher control costs and reduced stability. For Bernoulli control, the spectral radius ρ_B increases from 0.82 at 1 m to 3.3 at 10 m, indicating a decline in system stability as average SINR levels decrease. Furthermore, when the average SINR falls below a critical level, the packet reception probability drops below the critical control packet arrival probability, destabilizing the system.

Introducing a single intermediate hop between the controller and plant extends the range without compromising system stability. With a higher average SINR per hop, the multi-hop configuration enhances the system's ability to maintain stability. The ρ_B for Bernoulli control remains close to 1, indicating stability provided that hop distances are adequately managed. Markovian control shows even better stability, with spectral radius ρ_M consistently lower than ρ_B, though this comes at the cost of increased computational complexity due to the larger number of channel states.

Adding two intermediate hops further increases the transmission range without significantly compromising the average SINR. However, the total E2E delay rises notably, from around 6 ms in the one-hop to 30 ms in the three-hop case. In our MATLAB simulation, we use the maximum value of 3.2 ms for $T_{proc}(\ell)$. This increase in delay can impact time-sensitive control actions. The Bernoulli control strategy struggles to stabilize the system, as reflected by its higher ρ_B values, while the Markovian control strategy keeps the ρ_M below 1, ensuring stability. However, the added complexity from the increased number of channel states raises computational demands, making the Markovian model more challenging to implement in real-time systems. The rise in network latency further emphasizes the need for careful delay management.

Table I consolidates these observations by presenting the measured delay, cumulative distances, SINR values, and the spectral radius for both Bernoulli (ρ_B) and Markovian (ρ_M) control strategies. In this table, the first column shows the number of hops, the second column indicates the maximum delay observed, and the third column lists the cumulative distances over which measurements were taken. The fourth column reports the SINR values at these distances, while the fifth and sixth columns display arrays of spectral radius values for the Bernoulli and Markovian strategies, respectively. Notably, the use of ϵ in the spectral radius arrays signifies that the corresponding ρ values exceed 1, which implies that the control system is unstable under those conditions.

For example, in the single-hop configuration, both strategies maintain stability at shorter distances (with $\rho_B = 0.827$ and $\rho_M = 0.827$ at 1 m); however, at 8 m, as the SINR decreases, both spectral radii reach ϵ, indicating instability. In the two-hop configuration, the Bernoulli strategy remains stable ($\rho_B = 0.98$) at 8 m, but becomes unstable beyond 10 m, while the Markovian strategy manages stability over a longer distance, albeit at the cost of increased computational complexity. In the three-hop scenario, the Bernoulli strategy exhibits instability across all measured distances, whereas the Markovian strategy is able to stabilize the plant up to a certain range before its spectral radius again exceeds 1.

Overall, the results demonstrate that multi-hop configurations extend coverage and mitigate SINR degradation, thereby enhancing control stability when hop distances are well managed. However, they also incur higher end-to-end delays and increased computational complexity. Notably, the Bernoulli control strategy shows reduced stability, while the Markovian control strategy offers better performance under varying conditions, though with greater computational demands. These findings underscore a fundamental trade-off in multi-hop WNCSs between achieving extended coverage and maintaining stability, emphasizing the need for optimized hop selection and interference-aware scheduling to ensure reliable performance in industrial wireless networks.

V. Conclusion and Future Work

In this paper, we have extended an existing co-design framework for wireless network control systems (WNCSs) by incorporating multi-hop IEEE 802.15.4-based connectivity to address the limitations of direct communication over extended distances in industrial settings. Our analysis demonstrated that multi-hop configurations, by distributing the communication across shorter hops, can improve the SINR, which is crucial for maintaining stability and performance in industrial automation systems operating under Wi-Fi interference. However, while multi-hop links extend the operational range and enhance stability, they introduce additional network latency and computational complexity. Our simulations, comparing the Bernoulli and Markovian control strategies, reveal that while Markovian control provides superior stability under interference, it requires increased computational resources due to the need for a more detailed state-space analysis. Future work will explore dynamic routing for adaptive path selection under interference and node failures, alongside optimizing control strategies to balance computational demands and performance in multi-hop scenarios.

TABLE I
Comparison of delay, spectral radius, cumulative distance, and SINR in multi-hop settings

Hops	**Maximum Delay (s)**	**Cumulative Distances (m)**	**SINR (dB)**	ρ_B	ρ_M
1	0.0060	{1, 5, 8}	{9, 3, 1}	{0.827, 0.897, ϵ }	{0.827, 0.897, ϵ }
2	0.0184	{8, 10, 17}	{9, 5, -0.3}	{0.98, ϵ, ϵ }	{0.827, 0.83, ϵ}
3	0.0308	{17, 20, 22}	{5, 2, 1}	{ϵ, ϵ, ϵ}	{0.827, 0.83, ϵ}

Acknowledgment

Muhammed Azeem Khan is funded by the Swedish Knowledge Foundation through the International Research School in Transformative Technology.

References

[1] P. Park, S. C. Ergen, C. Fischione, C. Lu, and K. H. Johansson, "Wireless network design for control systems: A survey," *IEEE Commun. Surveys & Tuts.*, vol. 20, no. 2, pp. 978–1013, 2017.

[2] D. Baumann, F. Mager, U. Wetzker, L. Thiele, M. Zimmerling, and S. Trimpe, "Wireless control for smart manufacturing: Recent approaches and open challenges," *Proc. IEEE*, vol. 109, no. 4, pp. 441–467, 2020.

[3] Y. Zacchia Lun and A. D'Innocenzo, "Stabilizability of Markov jump linear systems modeling wireless networked control scenarios," in *58th IEEE Conf. Decision Control (CDC)*, 2019, pp. 5766–5772.

[4] A. Impicciatore, Y. Zacchia Lun, P. Pepe, and A. D'Innocenzo, "Optimal output-feedback control over Markov wireless communication channels," *IEEE Trans. Autom. Control*, 2023.

[5] Y. Ma, J. Guo, Y. Wang, A. Chakrabarty, H. Ahn, P. Orlik, X. Guan, and C. Lu, "Optimal dynamic transmission scheduling for wireless networked control systems," *IEEE Trans. Control Syst. Technol.*, vol. 30, no. 6, pp. 2360–2376, 2022.

[6] W. Liu, G. Nair, Y. Li, D. Nesic, B. Vucetic, and H. V. Poor, "On the latency, rate, and reliability tradeoff in wireless networked control systems for IIoT," *IEEE Internet Things J.*, vol. 8, no. 2, pp. 723–733, 2020.

[7] K. Gatsis, H. Hassani, and G. J. Pappas, "Latency-reliability tradeoffs for state estimation," *IEEE Trans. Autom. Control*, vol. 66, no. 3, pp. 1009–1023, 2021.

[8] M. Eisen, S. Shukla, D. Cavalcanti, and A. S. Baxi, "Communication-control co-design in wireless edge industrial systems," in *IEEE 18th Int. Conf. Factory Commun. Syst. (WFCS)*, 2022, pp. 1–8.

[9] D. Yang, Y. Xu, and M. Gidlund, "Wireless coexistence between IEEE 802.11- and IEEE 802.15.4-based networks: A survey," *Int. J. Distrib. Sens. Netw.*, vol. 7, no. 1, p. 912152, 2011.

[10] D. Chen, Y. Zhuang, J. Huai, X. Sun, X. Yang, M. A. Javed, J. Brown, Z. Sheng, and J. Thompson, "Coexistence and interference mitigation for WPANs and WLANs from traditional approaches to deep learning: A review," *IEEE Sensors J.*, vol. 21, no. 22, pp. 25 561–25 589, 2021.

[11] F. Zhang, F. Wang, B. Dai, and Y. Li, “Performance evaluation of IEEE 802.15.4 beacon-enabled association process,” in *22nd Int. Conf. Adv. Inf. Netw. and Appl.—Workshops (AINA Workshops)*, 2008, pp. 541–546.

[12] A. Gonga, O. Landsiedel, P. Soldati, and M. Johansson, “Revisiting multi-channel communication to mitigate interference and link dynamics in wireless sensor networks,” in *IEEE 8th Int. Conf. Distrib. Comput. Sens. Syst. (DCOSS)*, 2012, pp. 186–193.

[13] A. Saifullah, Y. Xu, C. Lu, and Y. Chen, “Real-time scheduling for WirelessHART networks,” in *31st IEEE Real-Time Syst. Symp.*, 2010, pp. 150–159.

[14] J. Chen, Q. Yu, Y. Zhang, H.-H. Chen, and Y. Sun, “Feedback-based clock synchronization in wireless sensor networks: A control theoretic approach,” *IEEE Trans. Veh. Technol.*, vol. 59, no. 6, pp. 2963–2973, 2010.

[15] L. Zhang, H. Gao, and O. Kaynak, “Network-induced constraints in networked control systems—a survey,” *IEEE Trans. Ind. Informat.*, vol. 9, no. 1, pp. 403–416, 2013.

[16] Y. Wang, M. C. Vuran, and S. Goddard, “Cross-layer analysis of the end-to-end delay distribution in wireless sensor networks,” *IEEE/ACM Trans. Netw.*, vol. 20, no. 1, pp. 305–318, 2012.

[17] D. E. Quevedo, A. Ahlen, and K. H. Johansson, “State estimation over sensor networks with correlated wireless fading channels,” *IEEE Trans. Autom. Control*, vol. 58, no. 3, pp. 581–593, 2013.

[18] J. Wu and T. Chen, “Design of networked control systems with packet dropouts,” *IEEE Trans. Autom. Control*, vol. 52, no. 7, pp. 1314–1319, 2007.

[19] Y. Zacchia Lun, C. Rinaldi, A. D’Innocenzo, and F. Santucci, “Co-designing wireless networked control systems on IEEE 802.15.4-based links under Wi-Fi interference,” *IEEE Access*, pp. 71 157–71 183, 2024.

[20] E. Sisinni, A. Saifullah, S. Han, U. Jennehag, and M. Gidlund, “Industrial internet of things: Challenges, opportunities, and directions,” *IEEE Trans. Ind. Informat.*, vol. 14, no. 11, pp. 4724–4734, 2018.

[21] M. Wollschlaeger, T. Sauter, and J. Jasperneite, “The future of industrial communication: Automation networks in the era of the Internet of things and industry 4.0,” *IEEE Ind. Electron. Mag.*, vol. 11, no. 1, pp. 17–27, 2017.

[22] S. Ghosh, S. Dey, and P. Dasgupta, “Pattern guided integrated scheduling and routing in multi-hop control networks,” *ACM Trans. Embedded Comput. Syst.*, vol. 19, no. 2, pp. 1–28, 2020.

[23] A. Aijaz and A. Stanoev, “Closing the loop: A high-performance connectivity solution for realizing wireless closed-loop control in industrial IoT applications,” *IEEE Internet Things J.*, vol. 8, no. 15, pp. 11 860–11 876, 2021.

[24] P. K. Mishra, D. Chatterjee, and D. E. Quevedo, “Stochastic predictive control under intermittent observations and unreliable actions,” *Automatica*, vol. 118, p. 109012, 2020.

[25] A. M. Girgis, J. Park, M. Bennis, and M. Debbah, “Predictive control and communication co-design via two-way gaussian process regression and aoi-aware scheduling,” *IEEE Trans. Commun.*, vol. 69, no. 10, pp. 7077–7093, 2021.

[26] R. Surender and P. Samundiswary, “Performance analysis of node mobility in beacon and non-beacon enabled IEEE 802.15.4 based wireless sensor network,” *Int. J. Comput. Appl.*, vol. 76, no. 12, 2013.

[27] G. F. Franklin, D. Powell, and M. L. Workman, *Digital Control of Dynamic Systems*, 3rd ed. Addison-Wesley, 1997.

[28] R. A. Horn and C. R. Johnson, *Matrix analysis*. Cambridge university press, 2012.